CRYSTAL STRUCTURE AND ANTIMICROBIAL ACTIVITY OF A HIGH SPIN COBALT(II) DIMER: $[CO_2(OH)_2 (AC)_3(BIPY)_2]\cdot K \cdot 2(H_2O)$

P. CORTES[a], A. M. ATRIA[b], M. T. GARLAND[c], R. BAGGIO[d], O. PEÑA[e], G. CORSINI[f]*

[a]Facultad de Ciencias Químicas y Farmacéuticas, Universidad de Chile. Santiago, Chile.
[b]Facultad de Ciencias Químicas y Farmacéuticas and CIMAT, Universidad de Chile. Santiago, Chile.
[c]Facultad de Ciencias Físicas y Matemáticas and CIMAT, Universidad de Chile. Santiago, Chile.
[d]Departamento de Física, Comisión Nacional de Energía Atómica. Buenos Aires, Argentina.
[e]L.C.S.I.M./UMR 6511CNRS/Institut de Chimie de Rennes, Université de Rennes I. Rennes, Francia.
[f]Laboratorio de Bacteriología Molecular, Facultad de Ciencias de la Salud, Universidad Diego Portales. Santiago, Chile.

ABSTRACT

The ionic cobalt (II) title complex $[Co_2(OH)_2 (Ac)_3(Bipy)_2]\cdot K \cdot 2(H_2O)$ (where Ac: Acetate, Bipy: 2,2-bipyridine) consists of anionic bimetallic unit in which cobalt ions are bridged by hydroxo and acetate ligands, balanced by a (disordered) potassium cation. The geometry at cobalt is distorted octahedral with the O atoms of a monodentate and a bridging acetate groups occupying the apical sites and O atoms from the hydroxo groups and N atoms from Bipy, the equatorial sites in each cobalt coordination sphere. Magnetic susceptibility data of powdered samples of the compound are presented.

The antimicrobial activities of the complex has been screened *in vitro* against the microorganisms *Staphylococcus aureus*, *Pseudomonas aeruginosa*, *Escherichia coli*.

Keywords: cobalt crystal structure, antibacterial activities.

INTRODUCTION

In recent years a substantial amount of work has been devoted to polynuclear complexes of transition metals, covering a very wide range of scientific interest, *viz*., in biology (since such systems have been suggested as synthetic models of the actives sites of metallobiomolecules), in materials science (the understanding of magnetic interactions in polynuclear complexes are one of the keys for the design of new and better materials of technological interest), etc [1-4].

Transition metal ions are also found in several bacterial species and are reported to play an important role in different enzymatic and physiological reactions [5]. An example is cobalt(II), metal cofactor of the coenzyme B12 and vitamin B12 [6] and their carboxylato-bridged complexes are taken as structural models of the active site in methionine aminopeptidase [7].

From the point of view of pharmacology cobalt complexes are also noted for their significant biological properties, namely antibacterial and antifungal activities [8-10].

In relation to the magnetic properties, the octahedral cobalt (II) systems are particularly difficult to forecast due to their dependence on several factors, like: i) the spin-orbit coupling which splits the ^4F ground terms of each Co(II) ion into two orbital triplets ($^4T_{1g}$ and $^4T_{2g}$) and one orbital singlet ($^4A_{2g}$), being the ground-state a multiplet; ii) the symmetry around the metal ion and iii) the Zeeman interaction [11].

As a part of a general project on transition metal compounds we have synthesized one such compound $[Co_2(OH)_2(Ac)_3(Bipy)_2]\cdot K \cdot 2(H_2O)$ (1) (Ac= acetate; Bipy= 2,2′-bipyridine). Here we report the single crystal structure and magnetic properties. The antimicrobial activity of this complex has been screened *in vitro* against Gram positive and Gram negative bacteria, by disc diffusion methods and the minimal concentration of the complex in order to inhibit the bacterial growth has been determined for all three strains.

EXPERIMENTAL

Reagents

Sodium acetate (Aldrich), 2,2′-bipyridine (Aldrich), cobalt (II) chloride (Aldrich) were used without further purification. The solvent (Fluka p.a absolute ethanol) was used as received.

Syntheses of the complex.

The complex was prepared by addition of 0.9237 mmol of sodium acetate and 1.5 mmol of 2,2-bipyridine to an ethanolic solution (20mL) of $CoCl_2\cdot 6H_2O$ (0.27 mmol). The resulting blue solution was stirred for ten minutes and then treated with $KClO_4$ (7.2 mmol), stirred for 24h and filtered. Single crystal were grown by slow evaporation of the resulting solution at room temperature. Elemental analysis (C,H,N) were performed on a Carlo–Erba EA 1108 Instrument.

Anal. Found: C: 43.32, H: 4.82, N: 7.21; Calc: C: 43.55, H: 4.36, N: 7.82

IR spectrum was recorded on a Bruker Spectrum IFS55 as KBr disc in the 4000-450 cm^{-1} spectral range .

Magnetic susceptibility measurements.

The magnetic susceptibility was determined over the temperature range 6-300K by using a SQUID magnetometer (QUANTUM DESING MODEL MPMS-XL5 instrument) with a field of 0.1T.

The data were corrected to compensate for the diamagnetism of the constituent atoms using the Pascal's constant.

Crystallography

Crystal data, data collection and refinements details for $[Co_2(OH)_2 (Ac)_3 (Bipy)_2]\cdot K \cdot 2(H_2O)$ are given in Table 1. The atomic coordinates and equivalent isotropic displacement parameter for all the atoms are given in Table 2.

A red parallelepiped crystal of (**1**) was mounted on a glass fiber and used for data collection.

e-mail: aatria@ciq.uchile.cl

Table 1. Crystal data and structure refinement for $[Co_2(OH)_2(Ac)_3(Bipy)_2]\cdot K\cdot 2(H_2O)$

Empirical formula	$Co_2 K N_4 O_{10} C_{26} H_{31}$
Formula weight	*716.306*
Crystal colour	*red*
Crystal size(mm)	*0.47 0.36 0.27*
Crystal system	*Triclinic*
Space group	*P1*
α (Å)	*9.0570 (17)*
β (Å)	*14.672 (3)*
χ (Å)	*15.735 (3)*
α (º)	*63.587 (3)*
β (º)	*80.985 (3)*
γ (º)	*71.815 (3)*
V(Å)^3	*1778.8 (6)*
Z,	*2*
D_{calcd} (Mg/m^3)	*1.338*
T (K)	297 (2)
λ (Å)	*0.71073*
μ (mm^{-1})	*1.101*
Scan mode	*phi and omega scans*
$2\theta_{max}$ (º)	*56.10*
Data $N_{collected}$ / N_{unique} / $N_{I>(I)?2}$	*14907 / 7673 / 5687*
R(int)	*0.0465*
h range	*-11 ⟶ 11*
k range	*-19 ⟶ 19*
l range	*-20 ⟶ 20*
Weighting scheme	*Rw=ſ² (Fo²)+[0.133(Fo²+2Fc²)/3] ²} -1*
F(000)	*736*
$[\Delta/\sigma]_{max}$	*0.011*
Nº of refined parameters	*411*
$[\Delta\rho]_{max}$ / $[\Delta\rho]_{min}$ (e Å^{-3})	*0.938 / -0.922*
S[a]	*1.049*
R[b] (obs., all data)	*0.0587, 0.0728*
R_w[c] (obs., all data)	*0.1903, 0.2004*

[a] $\Sigma = [\Sigma w (F_0|-|F_c|)^2/(N-P)]^{1/2}$, where P= number of parameters, and N= number of observed reflections

[b] $R = \Sigma ||F_0|F_c||/ \Sigma |F_0|$

[c] $R_w = [\Sigma w (|F_0|-|F_c|)^2/ \Sigma w|F_0|^2]^{1/2}$

Table 2. Fractional atomic coordinates and equivalent isotropic displacement parameters (Å^2) Ueq = (1/3) $\Sigma_i\Sigma_j U^{ij}a^i a^j a_i.a_j$.

	Occupancy	x	y	z	Ueq
Co1	1	-0.01024(6)	0.93327 (4)	0.78148 (3)	0.03567 (17)
Co2	1	0.14177 (5)	0.76801 (4)	0.94290 (3)	0.03350 (17)
K1A	0.814 (3)	0.3755 (3)	0.65184 (15)	0.65789 (16)	0.1395 (10)
K1B	0.186 (3)	0.3655 (15)	0.4887 (7)	0.5934 (7)	0.1395 (10)
O1	1	0.0711 (3)	0.91705 (19)	0.89170 (18)	0.0371 (6)
O2	1	0.0252 (3)	0.78566 (19)	0.84495 (18)	0.0385 (6)
N11	1	0.2228 (4)	0.6177 (2)	0.9883 (2)	0.0393 (7)
N12	1	-0.0371 (4)	1.0831 (3)	0.7122 (2)	0.0434 (8)
C11	1	0.1930 (5)	0.5596 (3)	0.9499 (3)	0.0534 (11)
H11	1	0.1311	0.5934	0.8968	0.064
C21	1	0.2522 (6)	0.4519 (3)	0.9876 (4)	0.0599 (12)
H21	1	0.2294	0.4128	0.9608	0.072
C31	1	0.3467 (5)	0.4015 (3)	1.0662 (3)	0.0582 (12)
H31	1	0.3878	0.3284	1.0930	0.070
C41	1	0.3788 (5)	0.4629 (3)	1.1044 (3)	0.0503 (10)
H41	1	0.4437	0.4314	1.1560	0.060
C51	1	0.3133 (4)	0.5704 (3)	1.0647 (3)	0.0397 (8)
C61	1	0.3315 (4)	0.6430 (3)	1.0998 (3)	0.0380 (8)
C71	1	0.4076 (5)	0.6144 (3)	1.1804 (3)	0.0503 (10)
H71	1	0.4564	0.5438	1.2170	0.060
C81	1	0.4107 (5)	0.6923 (4)	1.2066 (3)	0.0562 (11)
H81A	1	0.4605	0.6744	1.2615	0.067
C91	1	0.3377 (5)	0.7988 (3)	1.1493 (3)	0.0484 (10)
H91	1	0.3387	0.8523	1.1656	0.058
C101	1	0.2656 (4)	0.8220 (3)	1.0697 (3)	0.0416 (9)
H101	1	0.2184	0.8924	1.0314	0.050
N21	1	0.2599 (3)	0.7466 (2)	1.0442 (2)	0.0355 (7)
N22	1	-0.0900 (4)	0.9475 (3)	0.6692 (2)	0.0419 (7)
C12	1	0.0024 (5)	1.1435 (3)	0.7416 (3)	0.0506 (10)
H12	1	0.0525	1.1131	0.7990	0.061
C22	1	-0.0300 (7)	1.2514 (4)	0.6878 (4)	0.0710 (14)
H22	1	-0.0023	1.2937	0.7089	0.085
C32	1	-0.1037 (7)	1.2958 (4)	0.6025 (4)	0.0818 (17)
H32	1	-0.1266	1.3685	0.5661	0.098
C42	1	-0.1432 (6)	1.2335 (4)	0.5714 (4)	0.0692 (15)
H42	1	-0.1922	1.2629	0.5137	0.083
C52	1	-0.1089 (5)	1.1258 (3)	0.6274 (3)	0.0503 (10)
C62	1	-0.1378 (5)	1.0469 (3)	0.6029 (3)	0.0481 (10
C72	1	-0.2035 (5)	1.0673 (4)	0.5200 (3)	0.0618 (13)
H72	1	-0.2364	1.1364	0.4742	0.074
C82	1	-0.2192 (6)	0.9865 (5)	0.5066 (3)	0.0687 (15)
H82	1	-0.2638	0.9996	0.4515	0.082
C92	1	-0.1699 (6)	0.8860 (4)	0.5735 (3))	0.0624 (12
H92	1	-0.1801	0.8296	0.5647	0.075
C102	1	-0.1045 (5)	0.8685 (4)	0.6547 (3)	0.0524 (10)
H102	1	-0.0697	0.7996	0.7004	0.063
C13	1	0.3133 (4)	0.8452 (3)	0.7735 (3)	0.0416 (9)
C23	1	0.4657 (5)	0.8420 (4)	0.7172 (3)	0.0585 (12)
H23A	1	0.5483	0.8265	0.7571	0.088
H23B	1	0.4584	0.9094	0.6641	0.088
H23C	1	0.4866	0.7881	0.6946	0.088

Intensities were collected at room temperature on a Bruker AXS Smart Apex CCD diffractometer, using monochromatic Mo Kα radiation (λ=0.71069Å and a 0.3° separation between frames. For each one, data integration was performed using SAINT and a semi empirical absortion correction was applied using SADABS [12], both programs being including in the diffractometer package. The structure resolution was achieved by direct methods and difference Fourier .

H atoms attached to carbon were placed at their idealized positions (C—$H_{aromatic}$: 0.93, C—H_{methyl}: 0.96 Å) and allowed to ride. Methyl groups were allowed to rotate as well around the C—C axis. H atoms of hydroxo groups were located from the difference–Fourier syntheses and refined with restrained O—H:0.82(3) Å distances. All H atoms were assigned an isotropic displacement parameter $U_{isot}(H)=x.U_{equiv}(Host)$, with x=1.2 for aromatic and hydroxo H atoms and x=1.5 for methyl ones. The potassium

cation appears disordered into two sites of unequal populations (0.82:0.18), and the same happens with two hydration water molecules completing the structure, which appear split into three and four sites, respectively. The latter were refined using isotropic displacement factors, and their H atoms were not included in the model. Data collection: SMART–NT [13]. Cell refinement: SAINT–NT. Data reduction: SAINT–NT. Program(s) used to solve the structure: SHELXS-97 and program(s) used to refine the structure: SHELXL97 [14]. Molecular graphics: XP in SHELXTL/PC [15]. Software used to prepare material for publication: SHELXL97.

Antimicrobial activitiy.

Bacterial strains and media

Bacterial strains used in this study are property of the Molecular Bacteriology Laboratory collection (Universidad Diego Portales). *Staphylococcus aureus* AB68 and *Pseudomonas aeruginosa* SJD01 strains were obtained from Hospital San Juan de Dios (Chile) while the *Escherichia coli* BL21 strain was obtained from Novagen Inc.

Bacteria were grown in Mueller Hinton Broth and Mueller Hinton Agar (Difco). Cultures were incubated for 16 to 24 h at 37 ºC in an incubator or shaker, as required.

Antibacterial activity

The qualitative *in vitro* antibacterial activity of the complex was tested using the paper disc diffusion method [16]. The complex was dissolved in absolute ethanol and all the control discs were moistened with this solvent. The quantitative antibacterial activity of the cobalt complex was determined using minimal inhibitory concentration method (MIC) [17].

RESULTS AND DISCUSSION

Description of structure

Figure 1 presents a view of the complex, which core consists of two Co^{+2} cations bridged by two hydroxo groups and a (O,O´) bridging acetate, leading to a Co...Co distance of 2.786(1) Å. The remaining two acetato units are monodentate, binding through one of the carboxylato oxygen atoms, while making with the uncoordinated one strong H-bonds with the corresponding hydroxo hydrogen from the same side. The six fold coordination of the cobalt cations is completed by the (N,N´) bite of a chelating Bipy at each side of the complex.

Select bonds lengths and angles are listed in Table 3 and hydrogen-bond parameters are listed in Table 4.

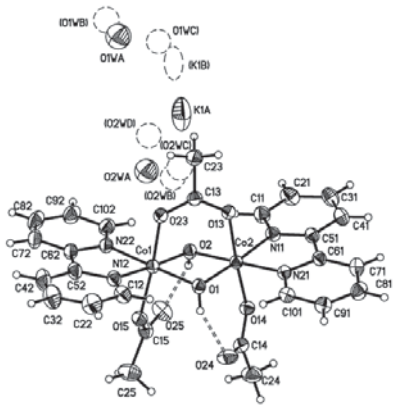

Fig. 1. XP diagram (Sheldrick, 1994) of (1), where non-disordered atoms as well as the main component of disordered ones have been drawn in full (40 % probability) displacement ellipsoids (Remaining ones as broken ellipsoids). In double broken lines, intramolecular H-bonds.

Table 3. Selected bond lengths [Å] and angles [°] for $[Co_2(OH)_2(Ac)_3(Bipy)_2]\cdot K\cdot 2(H_2O)$

Co(1)-O(1)	1.879(3)	Co(2)-O(2)	1.882(3)
Co(1)-O(2)	1.880(3)	Co(2)-O(1)	1.887(2)
Co(1)-O(23)	1.899(3)	Co(2)-O(14)	1.896(3)
Co(1)-N(22)	1.915(3)	Co(2)-O(13)	1.906(3)
Co(1)-O(15)	1.917(3)	Co(2)-N(21)	1.914(3)
Co(1)-N(12)	1.923(3)	Co(2)-N(11)	1.915(3)
$C(13)-O(13)_{coord}$	1.255(4)	$C(13)-O(23)_{coord}$	1.294(4)
$C(14)-O(14)_{coord}$	1.291(5)	$C(14)-O(24)_{uncoord}$	1.222(5)
$C(15)-O(15)_{coord}$	1.298(5)	$C(15)-O(25)_{uncoord}$	1.225(5)
Co(1)-Co(2)	2.7856(7)		
O(1)-Co(1)-O(2)	83.70(11)	O(2)-Co(2)-O(14)	89.96(12)
O(1)-Co(1)-O(23)	89.23(12)	O(1)-Co(2)-O(14)	97.39(12)
O(2)-Co(1)-O(23)	89.29(12)	O(2)-Co(2)-O(13)	90.06(12)
O(1)-Co(1)-N(22)	178.91(13)	O(1)-Co(2)-O(13)	88.51(12)
O(2)-Co(1)-N(22)	95.53(13)	O(14)-Co(2)-O(13)	174.06(11)
O(23)-Co(1)-N(22)	89.99(12)	O(2)-Co(2)-N(21)	178.59(12)
O(1)-Co(1)-O(15)	92.08(12)	O(1)-Co(2)-N(21)	97.88(12)
O(2)-Co(1)-O(15)	97.30(12)	O(14)-Co(2)-N(21)	89.32(12)
O(23)-Co(1)-O(15)	173.38(11)	O(13)-Co(2)-N(21)	90.54(12)
N(22)-Co(1)-O(15)	88.77(13)	O(2)-Co(2)-N(11)	95.75(12)
O(1)-Co(1)-N(12)	97.14(13)	O(1)-Co(2)-N(11)	176.37(13)
O(2)-Co(1)-N(12)	176.96(13)	O(14)-Co(2)-N(11)	86.13(12)
O(23)-Co(1)-N(12)	87.80(13)	O(13)-Co(2)-N(11)	87.95(13)
N(22)-Co(1)-N(12)	83.60(14)	N(21)-Co(2)-N(11)	83.00(13)
O(15)-Co(1)-N(12)	85.60(12)	Co(1)-O(1)-Co(2)	95.39(12)
O(2)-Co(2)-O(1)	83.41(11)	Co(1)-O(2)-Co(2)	95.55(12)

Table 4. Hydrogen bonds for $[Co_2(OH)_2(Ac)_3(Bipy)_2]\cdot K\cdot 2(H_2O)$ [Å and °].

D-H...A	d(D-H)	d(H...A)	d(D...A)	<(DHA)
O(2)-H(2)...O(25)	0.832(10)	1.91(2)	2.622(4)	143(3)
O(1)-H(1)...O(24)	0.813(10)	1.965(19)	2.664(4)	144(2)

The bridging acetate displays a clear resonance between coordinated oxygen atoms, with almost equal C—O distances, within experimental error. The monocoordinated moieties, instead, show off a very neat differentiation of *ca.* 6% between $C—O_{coord}$ (shorter) and $C—O_{uncoord}$ (longer) (See Table 3).

The Bipy units do not deviate significantly from planarity, with a mean departure of 0.04 (1) Å for unit 1 and 0.03 (1) Å for unit 2, leaving their respective cations 0.06 (1) and 0.02 (1) Å aside, respectively; that is to say, they coordinate in a straight fashion.

The $(Co^{+2})_2(C_2H_3O_2^{-1})_3(OH^{-1})_2(C_{10}H_8N_2)_2$ complex thus constituted behave as negatively charged ions, and due balance is achieved through the inclusion of one free (disordered) potassium cation for each anionic group, in a 2Co:1K ratio. The structure is completed by two (also disordered) hydration water molecules.

The structure presents a variety of non-bonding interactions, the most important is obviously the coulombian, which provides for the stabilizing long range order of the ionic groups; second in strength rank the couple of strong, molecular H-bonds providing for internal coherence within the complexes. But it is the much weaker π...π interaction between pyridinic groups the one which plays a leading role in organizing the (anionic) complexes into chains parallel to [11-1] and joining them together into a 3D bonded structure. Fig. 2 and Table 3 complement each other in presenting these results: Fig. 2 shows a simplified packing view, where only the schematized complexes have been represented.

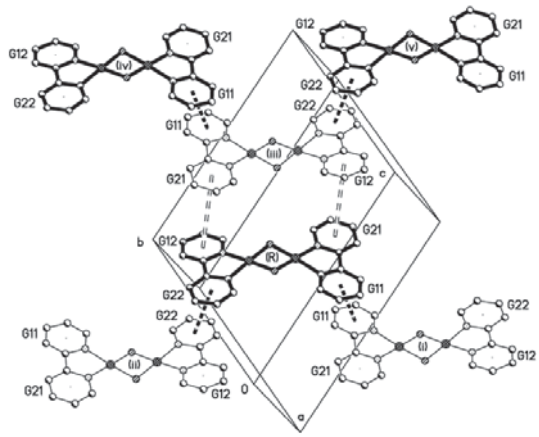

Fig. 2. Detailed view of a chain (running along [1¯11]) showing the main non-bonding interactions.

Chains run horizontally, and the stronger, intrachain π interactions are represented in heavy broken lines (First two entries in Table 4). Interchain interactions, in turn, are weaker and have been represented as double broken lines in Fig. 2 (Last two entries in Table 4). Finally, the cation and the hydration water molecules distribute in a disordered fashion filling the space between chains.

An almost exact replica of the complex herein reported but presenting cobalt (III) instead of cobalt(II) as metal centers has already been reported [18]. This introduces changes in the physico-chemical properties of the complex, mainly its ionic state, since the unit is now charged positively and therefore counterbalanced by an anion (perchlorate) instead of a cation (potassium) as in (**1**). Besides, in this cobalt(III) state of the ion no magnetic properties can be expected, in contrast to the case in (**1**). These differences, however, do not show up at all in the structure of the binuclear units, which superinpose almost exactly into each other with an average misfit of 0.099 (5) Å.

The present structure (1) is also similar to the $[Co_2(\mu\text{-}OH)_2\ (\mu\text{-}Oac)(OAc)_2\ (bpa)_2]OAC\ 4{\cdot}H_2O$ **(2)**, where bpa is 2,2 bipyridylamine and OAC is acetate [19]. In this compound each Co(III) center is coordinated by two pyridyl N atoms of the terminal bpa ligand (in trans-trans mode) and four oxygen. The distances are Co(1)-N(3)=1.934 Å, Co-N(1)= 1.937 Å, Co-O(3)=1.907Å, Co-O(5)=1.898 Å and Co-$O(1)_{OH}$ =1.894 Å, Co-$O(2)_{OH}$=1.894 Å.

In this complex (**2**) all the Co–ligand bond legths are slightly longer than the corresponding distances found for **(1)**

IR Spectrum

The IR spectrum of the compound (**1**) show a broad band at 3460, 3467 and 3449 cm^{-1} respectively which can be assigned to the bridging OH vibration of the hydroxo bridge and /or lattice water.

The spectrum also exhibit the broad and intense band at 1570 cm^{-1} correspond to the $\gamma_{as}(COO^-)$ vibration and a medium broad band at 1435 and 1434 cm^{-1} correspond to the bidentate bridging coordination mode of the carboxylate group within a binuclear specie.

Magnetic properties

The cobalt (II) cation has the $3d^7$ configuration and, under O_h symmetry, it possesses the $^4T_{1g}$ ground state. Magnetic data of a powdered sample of (I) were collected in the temperature range of 6–300K.

The results are shown in Fig. 3. The behaviour of the magnetic susceptibility can be well described in the range 20-300 K by the Curie-Weiss law $\chi_M = C/(T-\theta)$, with a negative temperature intercept θ="11,26 K and a slope corresponding to a Curie constant of 5.27 cm^3 K mol^{-1}.

The χ_M T product of the complex decreases slowly from 5.07 to 4.39 $cm^3K\ mol^{-1}$ in the 300-60K region. The decrease is slightly more pronounced below 55K, until it reaches 3.49 $cm^3K\ mol^{-1}$ at 6K. The observed magnetic moment value for cobalt(II) at room temperature is μ = 4.50 BM. This value lays midway the "spin only" value of high spin cobalt(II) (3.87 BM, $\mu_{o.s}=[4S(S+1)]^{1/2}$; S = $^3/_2$), and the expected one when the spin and orbital moment exist independently (μ = 5.20 BM; $\mu_{LS} = [L(L+1) + 4S(S+1)]^{1/2}$, L = 3, S = $^3/_2$). This might indicate either a contribution of the orbital angular moment to the magnetic moment.

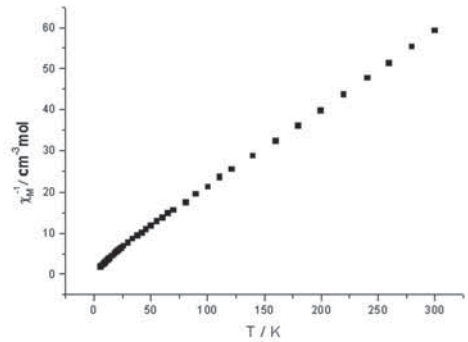

Fig. 3. Inverse of the magnetic susceptibility (χ_M^{-1}) as a function of temperature.

Screening for antimicrobial activities

The *in vitro* biological screening effects of (1) were tested against Gram positive (*Staphylococcus aureus*) and Gram negative (*Pseudomonas aeruginosa* and *Escherichia coli*) bacteria.

Qualitative assays using paper disc diffusion methods showed that the cobalt (II) complex presented antibacterial activity over both types of bacterial strains (Gram positive and Gram negative) where commercial antibiotics did not; in fact, the clinical isolated strains under examination of *Staphylococcus aureus* proved to be resistant to cephalosporins as cefazolin and cefotaxime, while those of *Pseudomonas aeruginosa* showed to be resistant to Imipenem (carbapenems type antibiotics). All these bacteria, however, when exposed to the action of the cobalt complex under study presented a significant sensitivity as suggested by the inhibition zone diameters in the paper disc diffusion assays (Shown in Table 5), which seem to point to *Pseudomonas aeruginosa* as the one to be more sensitive the cobalt complex action. The closeness of the results, however, obtained through a strictly qualitative method like paper disc diffusion, precluded a definite assessment for that a quantitative experiment was set up looking for the MIC of the compound under study against the growth of the microorganisms tested in this paper. The final results are also quoted in Table 4, and they definitely confirm *Pseudomonas aeruginosa* as the most sensitive of the three strains tested, with a significantly lower concentration required for growth inhibition (375 μg/μL, against 500 μg/mL for the other two). Results for *Staphylococcus aureus* and *Escherichia coli,* in turn, do not show significant differences with each other within experimental error.

Table 5. Antibacterial activity of $[Co_2(OH)_2(Ac)_3(Bipy)_2]\cdot K\cdot 2(H_2O)$

Bacterial strains	Zone of inhibition (mm)*	MIC** (μg/mL)
Staphylococcus aureus AB68	12	500
Escherichia coli BL21	11	500
Pseudomonas aeruginosa SJD01	13	375

* Used disk with 600 μg of $[Co_2(OH)_2(Ac)_3(Bipy)_2]\cdot K\cdot 2(H_2O)$ complex. Number of assays = 3, estimated error ± 1 mm.

** MIC is the minimal drug concentration required to inhibit bacterial growth. Number of assays = 3.

CONCLUSIONS

A dimeric cobalt(II) complex has been synthesized, and characterized by single crystal X-ray structural analysis and magnetic susceptibility measurements.

Both techniques provided interesting, though not completely unexpected results.

In constrat of geometric features such as acetate and hydroxo bridges this complex exhibit a simple paramagnetic behaviour probably due to poor overlap between the magnetic molecular orbital of the two metals ions through this bridges.

However, the fact that the compound presents an antibiotic activity against resistant strains might have profound biotechnological and medical implications, for what the action mechanisms involved and potential *in vivo* effects will be the subject of further studies.

ACKNOWLEDGEMENT

This research was supported by DI, Universidad de Chile (Project ENL 05/13). We are also grateful to Region de Bretagne. We acknowledge the Spanish Research Council (CSIC) for providing us with a free-of-charge license to the CSD system. P.C. acknowledges to Proyecto MECESUP UCH-0116 for a doctoral scholarship.

REFERENCES

[1] Hay, D. J., Thibeault, J. C. & Hoffmann., R. J. Am. Chem. Soc. 97, (1975). 4884.
[2] Willet, R. D., Gastteschi, D. & Kahn, O., Editors. Magneto-Structural Correlation in Exchange Coupled System. NATO ASI Series D. Reidel Publishing Co. Dordrecht, Holland, (1984).
[3] Holm, R. H., Kennepont, P. & Solomon, E. I. J. Chem. Rev. 96, (1996),2239.
[4] Lippard, S. J. & Berg, J. M. Principles of Bioinoganic Chemistry. University science Books Mill Valley (1994).
[5] Davies B.D., DulberccoH.N., Eiser H.S.,Ginsberg W.B. Wood and Mecarty. Microbiology 2nd. Ed. Haarper and Taw. London (1973).
[6] Fraústo da Silva, J. R. & Williams, R. J. P. The Biological Chemistry of the Elements. Clarendon Press. Oxford (1997).
[7] Roderick, S. L. & Matthews B. W. Biochemistry 32, (1993). 3907
[8] Nomiya K., Yoshizawa A., Yoshizawa K., Yoshizawa K., Yoshizawa N., Yoshizawa S., Watanabe J. Journal of Inorganic Biochemistry 98 (2004) 46.
[9] Bellú S., Hure E., Frappé M.,Trossero C., Molina G., Drogo C., Williams P., Atria A.M., Muñoz J.C.,Zacchino S., Sortino M., Campanogli D., Rizzotto M. Polyhedron 24, 4, (2004) 501.
[10] Jiménez-Garrido N., Perelló L., Ortiz R., Alzuet G., González-Alvarez M., Cantón E., Liu-González M., García-Granda S., Pérez-Priede M. Journal of Inorganic Biochemistry 99, (2005) 677.
[11] Kahn, O. Molecular Magnetism .VCH publishers. New York (1993).
[12] Sheldrick, G. M. SADABS. Multi-Scan Absorption Correction Program. University of Göttingen (2001).
[13] Bruker. SAINT. Version 6.02a. Bruker AXS Inc., Madison, Wisconsin, USA. (2000)
[14] Sheldrick, G. M. SHELXS-97 and SHELXL97 Programs for Structure Resolution and for Structure Refinement, University of Göttingen, Germany. (1997)
[15] Sheldrick, G. M. SHELXTL-PC. version 5.0 Siemens Analytical X-ray Instruments, Inc., Madison, Wisconsin, USA. (1994)
[16] Liu, K. Kwasniewska, Bull. Environ. Contam. Toxicol. 27 (1981) 289.
[17] National Committee for Clinical Laboratory Standards. *Methods for Dilution Antimicrobial Susceptibility Tests for Bacteria That Grow Aerobically—Fifth Edition: Approved Standard M7-A5*. NCCLS, Wayne, PA, USA. (2000).
[18] Dimitrou, K., Folting, K., Streib, W. E. & Christou, G.. J. Am. Chem. Soc., 115, (1993),6432.
[19] Du, M., Zhao, X. J. Acta Cryst. E60, (2004), m785.